Journal of University of Babylon, Engineering Sciences, Vol(26), No(4): 2018.

Modeling and Optimization of Bobbin Friction Stir Welding for AA6061-T6 alloy Utilizing Response Surface Methodology

Samir Ali Amin
Mechanical Eng Dept. , University of Technology
alrabiee2002@yahoo.com
Mohannad Yousif Hanna
Mechanical Eng. Dept. , University of Technology
mohannad_hanna@yahoo.com
Alhamza Farooq Mohamed
Mechanical Eng. Dept. , University of Technology
alhamza88f@yahoo.com

Abstract

Bobbin friction stir welding (BFSW) is special kind of friction stir welding. This investigation aims to develop empirical models through mathematical relationships between the welding process parameters and mechanical properties of Aluminum alloy AA6061-T6 welded joint created by using bobbin tool and to find the optimum welding parameters. The welding speed range (40-200 mm/min) and rotational speed range (340-930 rpm) were utilized (as the used input factors) to find their effects on elongation, tensile strength and maximum bending force as the main responses. These models were built using Design of Experiment (DOE) software 'version 10' with Response Surface Methodology (RSM) technique. The models adequacy were tested via the (ANOVA) analysis. The obtained models appeared that as the welding speed or rotational speed increases, the elongation, tensile strength and maximum bending force of the welded joint firstly rise to a maximum value and then drop. The optimum welding parameters were rotational speed (623.949 rpm) and welding speed (128.795 mm/min) with (6.33%), (204 MPa) and (6.216 KN) of elongation, tensile strength and maximum bending force, respectively. A proper harmonization was obtained between the models predicted results and the optimized ones with actual trial with 95% level of confidence.

Key words: Bobbin FSW, Response Surface Methodology, Modeling and Optimization.

الخلاصة

اللحام بالخلط الاحتكاكي نوع (bobbin) نوع خاص من اللحام بالخلط الاحتكاكي. تهدف هذه الدراسة الى عمل نماذج تجريبية من خلال علاقات رياضية بين عوامل اللحام و الخواص الميكانيكية لوصلات اللحام لسبيكة المنيوم (AA6061-T6) تم لحامها بأداة لحام نوع (bobbin) و أيجاد عوامل اللحام المثالية. مديات للسرعة الدورانية هو (340–930 دورة/دقيقة) ولسرعة اللحام هو (40–200 ملم/دقيقة) والتي استخدمت كعوامل ادخال للحصول على تأثيرها على الاستطالة، مقاومة الشد و اقصى قوة انحناء بوصفها الاستجابات الرئيسية. هذه النماذج اسست على منهجية الاستجابة السطحية (RSM) في برنامج التصميم التجريبي "الاصدار العاشر". باستعمال تحليل التباين (ANOVA) تم التأكد من صلاحيتها. هذه النماذج اظهرت بانه عند زيادة سرعة اللحام او السرعة الدورانية فأن الاستطالة، مقاومة الشد و قوة الانحناء القصوى تصل الى اقصى قيمة في البداية ومن ثم تقل. كانت عوامل اللحام المثالية هي(623.949 دورة/دقيقة) للسرعة الدورانية و (128.795 ملم/دقيقة) للخطية مع استطالة (6.33%) و مقاومة شد (204 ميكا باسكال) و أقصى قوة انحناء (6.216 كيلو نيوتن). وجد توافق جيد بين النتائج المتحصلة من النماذج الرياضية والتجريبية عند العوامل المثالية بمستوى ثقة 95%.

الكلمات المفتاحية: لحام الخلط الاحتكاكي، منهجية الاستجابة السطحية,النمذجة و الأمثلية.

1. Introduction

Friction stir welding process (FSW) is a solid state bonding technique that was feigned at The Welding Institute (TWI), in 1991. It is a substitutional welding technology to conventional fusion welding. The joint is produced via a non-consumed refractory cylindrical rotating tool, mechanically passed through the material of the

work-piece. The friction between wear-resistant tool and the substrate generates heat. Because the frictional heat is generated, the stirred material is softened and mixed (Kumbhar and Bhanumurthy, 2008). Since the material of the work-pieces does not reach to melting point, the bonding is deemed a solid-state process. Nevertheless, the grains are relocated and dynamically recrystallized. Under the shoulder of the tool, the material flows are like the forging process, whereas the material flows around the probe of the tool are similar to the extrusion process (Mishra and Ma, 2005).This technique is used for joining aluminum alloys, although other materials are possible inclusive dissimilar materials. The welding technology, patented via Thomas et al. has been used to automotive, shipbuilding, and aerospace industries (Seud and Pons, 2016).

The usage of bobbin tool, as known bobbin friction stir welding (BFSW), see figure (1), presented the capability to outdo certain restrictions met in traditional friction stir welding (Mishra *et.al.,* 2014). The operation is preceded by a certain tool consisting of a probe and a pair of shoulders. The tool is in touch with the lower and upper surfaces of substrate. It can be referred to that the Aluminum alloy plates with a higher thickness can be joined by friction stir welding process; nevertheless, the coming information show why it's eligible to use the bobbin tool for this intent as well. Using two shoulders helps to balance the down forces created via the separated shoulders of tool and so revokes the net down force. And, peril of root flaws is basically removed by like a design of tool. Due to the balanced profile of heat input, the bobbin friction stir welding process exhibits good weld joints with too lower cross-seam distortions than friction stir welding process. Furthermore, this technique can rise the speed of welding, and so raise efficiency of the welding operation in substrate with a higher section thickness (Threadgill *et.al.,* 2010).

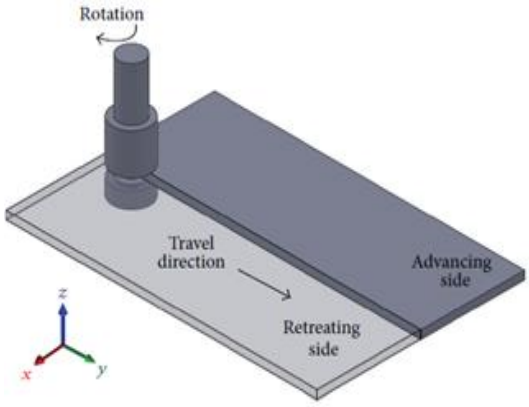

Figure 1: Schematic diagram of BFSW (Seud and Pons, 2016).

The soften part consisting of the weld stir zone (WSZ), the thermal mechanically affected zone (TMAZ) and the heat affected zone (HAZ) is generated due to the impairment (dissolution or coarsening) of strengthening precipitates resulted by thermal cycles of the FSW (Mishra and Ma, 2005; Fonda and Bingert, 2004). This caused a reduction in the ultimate tensile strength compared to base material. To enhance the properties of the welded joint via controlling the peak temperature level and the cooling rate during BFSW, so the optimization of the process parameters is so important.

Many of previous researches (Seud *et.al.,* 2014, Li *et.al.*, 2014, Zhang *et.al.*, 2015 ; Wang *et.al.*,2015) have highlighted the understanding the influence of bobbin friction stir welding process (tool design and process parameters) on the behavior of material flow, microstructure and mechanical properties of the welded joints, but there

is a very few investigations dealt with modeling and optimization of BFSW process. While, this subject has a large active area in CFSW. (Jayaraman *et.al.*,2009) determined the influence of process variables, like rotational speed, traverse speed, and downward axial force on the ultimate tensile strength and optimized the process variables of friction stir welded RDE-40 aluminum alloy using Taguchi approach. (Ghetiya and Patel , 2014) developed artificial neural network (ANN) depending on back (BP) of error prognosis of the tensile strength in FSW of aluminum alloy AA8104 plate. The input variables of the model comprise of tool rotational speed, welding speed, axial force and shoulder diameter, whilst the response of the model is the ultimate tensile strength of the welded joint. (Samir *et.al.*, 2015) developed an empirical modeling as a mathematical relationship between elongation, tensile strength and maximum bending force and welding parameters of FSW of AA2024-T351 and determined the optimum parameters of the process to obtain the maximum properties of welded joints. Response surface methodology (RSM) was used. (Trueba *et.al.*, 2017) found the relationship between welding temperature, void generation and mechanical properties and the welding parameters and obtained the optimum parameters for self-reaction FSW of AA6061-T6 plate using a factorial design. The evaluated parameters were traverse and rotational speeds and plunge force of the tool.

Response surface methodology (RSM) is a set of mathematical and statistical techniques, which are utilized for building empirical modeling and analysis of cases, in which a response of interest is affected via sundry parameters, and the aim is to optimize this response (Montgomery , 2000).

In the present work, an investigation has been performed to establish empirical mathematical models between the mechanical properties (elongation, tensile strength and maximum bending force) and welding parameters (welding speed and rotational speeds) of bobbin friction stir welded AA6061-T6 using the RSM technique. Also, this work aims to determine the optimum process parameters for higher mechanical properties of the welded joint by employing a numerical optimization method.

2. Experimental Work:

In this work the base metal was aluminum alloy AA6061-T6.The plate of AA6061-T6 was cut into the desired size (200 mm x 100 mm x 6.25 mm) via a power saw cutting machine, and the edge of the piece was ground to secure that there is no chasm exists between the two substrates that make the desired butt joint design. The chemical analysis of used material was obtained via a spectra device available in the Special Institute for Engineering Industries (SIEI), as presented in table (1). The mechanical properties were performed for this plate in strength laboratory in Mechanical Engineering Department, University of Technology are given in table (2). A bobbin tool of straight cylindrical with four flat surfaces probe profile and flat shoulders was used. The diameter of the probe and shoulder were 8 and 24 mm, respectively. The shoulders gap was equal to plate thickness (6.25 mm), while the flat side width was 0.5 mm, see figures (2) and (3). The tool in this work was fabricated from a hot-work tool steel (H13) with a chemical composition given in table (3). The tool had been heat treated resulting in about 49 HRC (ASM, Vol. 4, 1991). The flat feature on the probe can cause a horizontal flow which helps in stirring the soft material, while the fit gap between the shoulders of the tool and substrate thickness can be provided a vertical flow movement of soft material because of the used plate here was not thick (Seud *et.al.*, 2014). The range of rotational speeds (spindle speed) used for the welding experiments was (340 to 930) rpm, whereas the welding speed (traverse speed) range was (40 to 200) mm/min. Classic milling machine model (FU

251) was used to complete the welding process. An image of the milling machine is shown in figure (4). The specifications of the milling machine are: 4 K.W, 1.5 K.W, 40-2000 rpm and 12.5-630 mm/min for main drive electric motor, feeding drive electric motor, spindle speed and feeding rate respectively. The welding process direction was perpendicular to the direction of the rolled aluminum plates, see figure (5).

Table 1: Chemical compositions of the actual and standard aluminum alloy 6061-T6

Element	Si	Fe	Cu	Mn	Wt% Mg	Cr	Zn	Ti	Ni	Al
Standard **(ASTM B209)**	0.4-0.8	< 0.7	0.15-0.4	< 0.15	0.8-1.2	0.04-0.35	< 0.0.25	< 0.7	< 0.05	Bal.
Actual	0.6	0.57	0.26	0.10	0.89	0.18	0.037	0.054	0.003	Bal.

Table 2: Mechanical properties of the actual and standard aluminum alloy 6061-T6

Property	Yield stress (MPa)	Ultimate tensile stress (MPa)	Elongation (%)
Standard Value **(ASTM B209)**	≥ 240	≥ 290	≥ 10
Actual Value	244.5	295	11.5

Table 3: Standard and actual chemical compositions of hot-work tool steel (H13)

Element	C	Si	Mn	Wt% P	V	S	Cr	Mo	Fe
Standard **(ASTM, A681-94)**	0.32-0.45	0.8-1.25	0.2-0.6	< 0.03	0.8-1.2	< 0.03	4.75-5.5	1.1-1.75	Bal.
Actual	0.35	1.05	0.3	0.01	1.01	0.006	5.01	1.23	Bal.

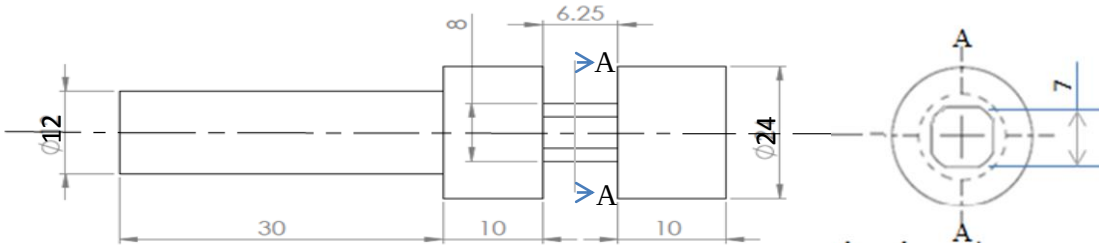

Figure 2: Drawing of used BFSW-Tool (all dimensions in mm)

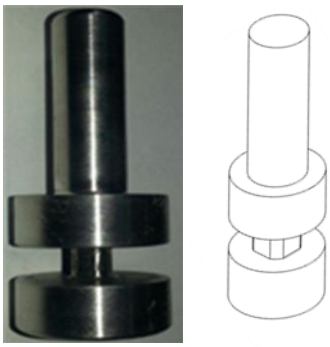

Figure 3: Used BFSW-Tool

Figure 4: Classic milling machine used for BFSW process

Figure 5: The procedure of the welding process

Tensile test was done on specimens possessed in a normal direction to the welding line to define the tensile properties of the joints for all welding experiments. The shape and dimensions of longitudinal tensile specimens consistent with the standard **(ASTM E-8M)** are presented in figure (6.a). All tensile tests were done at room temperature and constant loading rate (1 mm/min) using a computerized universal testing machine (Hydraulic Tunis Olsen). And, the average value of three tensile tested samples was taken for determining the elongation and ultimate tensile strength of each joint. Three point bending test was done to obtain the maximum bending force of the joints. The shape and dimensions of the longitudinal bending sample according to the standard **(ASTM E-190M)** are presented in figure (6.b). The bending test was done at a constant loading rate (5 mm/min) at room temperature by a universal testing machine (Hydraulic LARYEE testing machine).

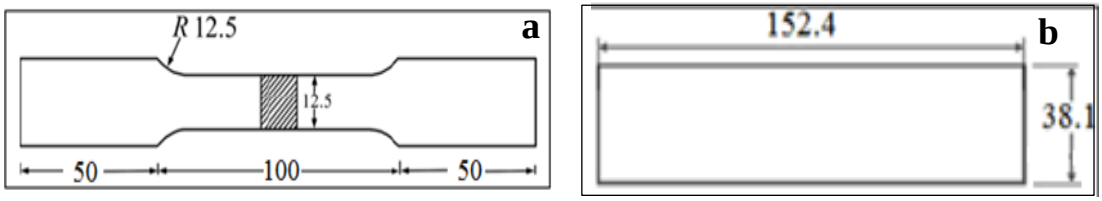

Figure 6: a) Tensile test specimen (all dimensions in mm) (ASTM E-8M) b) Bending test specimen (all dimensions in mm) (ASTM E-190M)

3. Experimental Design Matrix

In the entire experimentation, the used input parameters were chosen depending the pervious researches, investigated expertise, and the limitation of experimental records. In this paper, RSM employing a central composite rotatable design (CCD) for two factors (two inputs for three outputs) with 5 central points (0) and (α) approach was employed. Thus, each input factor was utilized at various coded levels of +2, +1, 0, -1, and -2, where every level employed matched to actual value tantamount to coded one. Table (4) lists the input factors with five levels.

In this research, the experimental design matrix comprised of 13 trials (runs). The runs were carried out at random employing the run order for one state depending on welding speed and rotational speed; these runs are listed in the table (5).

Table 4: Used levels of input factors

Input factor	Levels				
	- 1	+ 1	0	- 2	+ 2
Rotational speed (rpm)	430	730	560	340	930
Welding speed (mm/min)	80	160	125	40	200

4. Results and Discussion

4.1 Results of Mechanical Tests

After implementing the trials, the obtained welded joints were visually inspected and the welds with acceptable appearance (without defects) were selected, see figure (7). Then, the mechanical tests were carried out, as shown in the figures (8) and (9). The obtained data of elongation, tensile strength and maximum bending force are given in table (5) as output factor according to the experimental design matrix.

Table 5: Input factors and outputs matrix design

Std. No.	Run No.	Rotational speed (rpm)	Weling speed (mm/min)	Elongation (%)	Ultimate tensile stress (MPa)	Maximum bending force (KN)
1	11	430	80	4.31	166.0	5.10
2	13	430	160	4.86	176.5	5.52
3	2	730	80	5.08	185.0	5.75
4	8	730	160	5.95	200.0	6.10
5	4	340	125	4.00	164.0	5.00
6	3	930	125	3.55	183.0	5.60
7	10	560	40	2.34	141.0	4.50
8	6	560	200	4.00	170.0	5.40
9	9	560	125	6.75	198.0	6.20
10	7	560	125	6.55	198.0	6.00
11	1	560	125	7.00	201.0	6.00
12	5	560	125	7.00	202.0	6.00
13	12	560	125	6.70	203.0	6.20

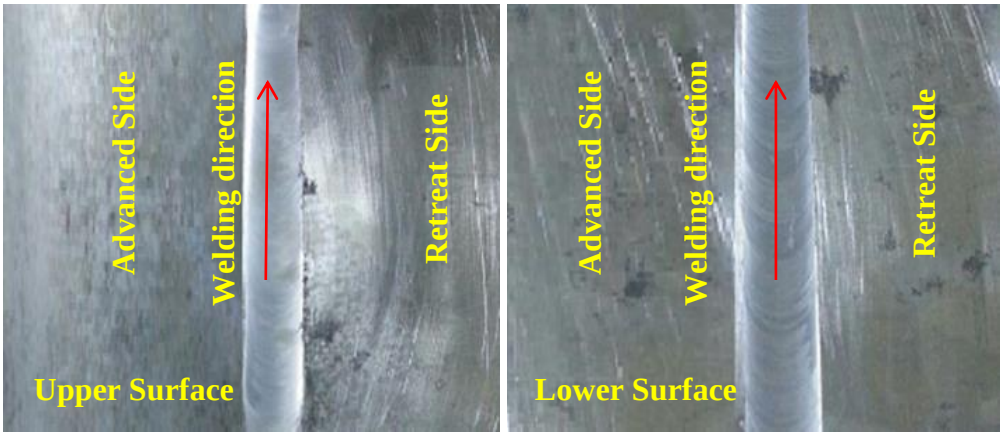

Figure 7: Successful welded joint

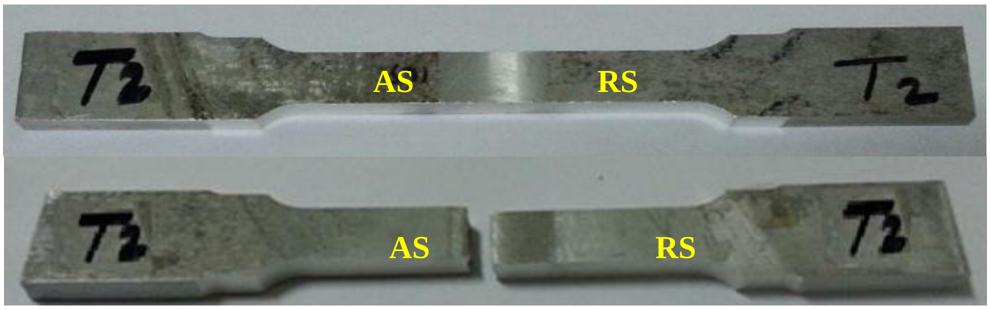

Figure 8: Tensile test welded specimen

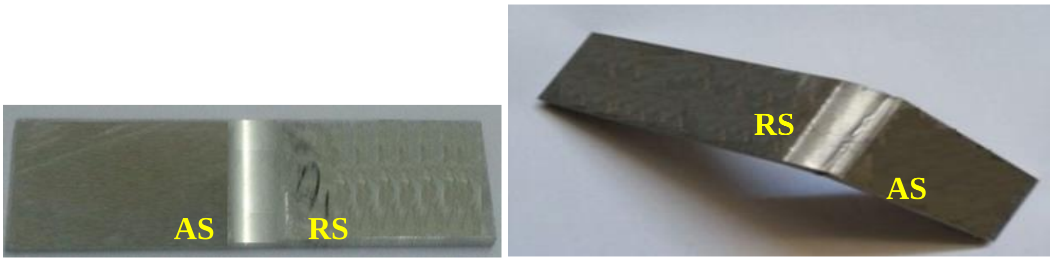

Figure 9: Bending test welded specimen

4.2 Modeling of the Elongation

For the elongation, the (ANOVA) analysis for the response surface quadratic model was completed to statistically analyze the outcomes, as listed in table (7). The model F-value of (270.53) in this table reveals that this model is significant. Values of "Prob > F" less than 0.05 show that the model terms are considerable. In this state, A, B, A^2 and B^2 are important model terms. Subsequently, the rotational speed (A), welding speed (B), squared rotational speed (A^2) and squared welding speed (B^2) have significant impact on the elongation. Because of the lack of fit is trivial (with P-value higher than 0.05), so this model is useful with 95% confidence. Consequently, the experiment quadratic predicted model evolved for the elongation of joint welded by BFSW tool is given in terms of actual Factors as follows:

$$\text{Elongation} = -6.54781 + 0.045380 * A + 0.14480 * B - 3.63735E-005 * A^2 - 5.62014E-004\ B^2 \qquad (1)$$

Table 6: ANOVA analysis for Response Surface Reduced Quadratic Model for Elongation

Source	Sum of Squares	Degrees of freedom	Mean Square	F Value	p-value Prob > F
Model	28.00	4	7.00	270.53	< 0.0001 significant
A-Rotational speed	2.15	1	2.15	82.94	< 0.0001
B-Welding speed	1.89	1	1.89	73.12	< 0.0001
A^2	13.98	1	13.98	540.31	< 0.0001
B^2	18.43	1	18.43	712.53	< 0.0001
Residual	0.21	8	0.026		
Lack of Fit	0.052	4	0.013	0.34	0.8425 not significant
Pure Error	0.15	4	0.039		
Cor Total	28.20	12			
Std. Dev.	0.16		R-Squared		0.9927
Mean	5.24		Adj R-Squared		0.9890
C.V.	3.07		Pred R-Squared		0.9880
PRESS	0.50		Adeq Precision		34.367

The diagnostic inspection of the model was performed by utilizing residual analysis, and the consequences are shown in the figures (10) and (11). The graph of normal probability for elongation is depicted in the figure (10). This figure appears that the residuals locate on a straight line revealing the normal distribution of errors. Figure (11) presents the standardized residuals versus the predicted values. These residuals appear that there is no any evidence of unusual modality and they distribute in both negative and positive sides. That reveals the accuracy of model, and there is no reason to think about any contravention of the assumption of independence or constant variance. Also, figure (12) manifests that the predicted data of elongation are near to actual that were obtained from the trials, denoting a good harmonization between the predicted and experimental outcomes. As regards the individual influence of each input parameter deviated from the center point of the selected level, figure (13) indicates the perturbation of elongation in this model. Figure (14) offers the 2D contour plot of rotational and welding speeds and elongation as a response. It is confirmed that the result as a function of the welding and rotational speeds. At first, the increasing in the rotational speed leads to increase the elongation, then it is decrease with the increasing the speed. This conductance also applies on the welding speed. Figure (15) depicts the 3D plot of welding parameters effect on elongation, it can be noted that the welding and rotational speeds have the seam effective. Higher rotational (spindle) speed (930 rpm) produces higher heat input (frictional heat generation) per unit length, and the decrease of cooling rate in the BFSW gives rise to immoderate grain growth, which subsequently lead to reduce the properties of the welding zone. This interpretation is compatible with other researches **(Zhou *et.al.*, 2017)**. The grains with smaller size will oblige more constraints to the movement of dislocation and own greater impedance to the localized plastic deformation **(Sato and Kokawa, 2001)**. Internal void (tunnel defect) produced at lower rotational speed (340 rpm), see figure (16.a). At (340 rpm), rotational speed resulted a lack in stirring due to the lower heat input, which resulted in inadequate plastic deformation that produced lower mechanical properties in the welded joint. The mechanical properties increased when the welding speed was increased from 40 to 125 mm/min, see figure (16.b), and then reduce due to the formation tunnel defect in the welded joint with increasing the welding speed to 200 mm/min, see figure (16.c). The influence of welding speed is consistent with previous researches **(Cevik *et.al.*, 2016, Liu *et.al.*, 2013)**. Lower welding speed causes higher heat input and gives rise to immoderate grain growth, which subsequently lead to slash the properties of the welding zone. While, higher welding speed produces insufficient generation of heat. So, 125 mm/min results sufficient heat generation and that is enough to cause the metal to flow plastically.

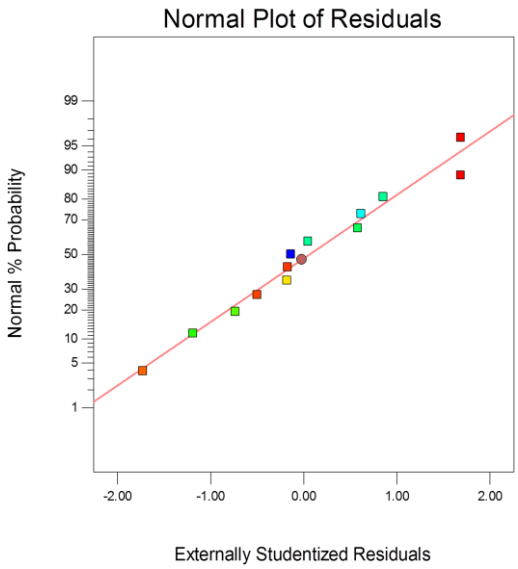

Figure 10: Normal probability for elongation data

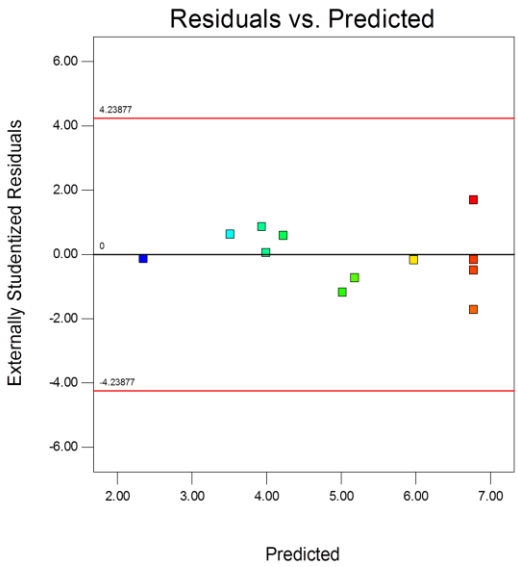

Figure 11: Residual versus predicted output elongation data

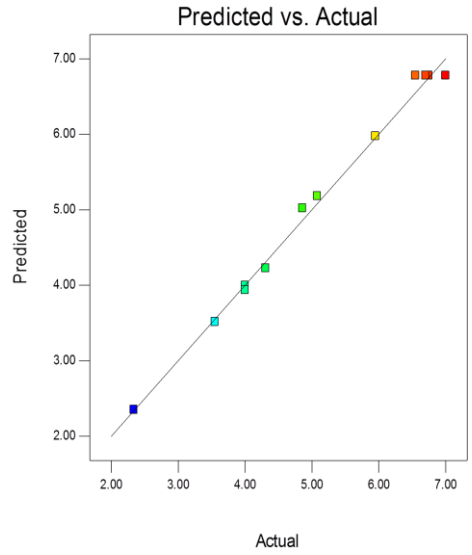

Figure 12: Predicted versus actual showing the elongation data for comparison

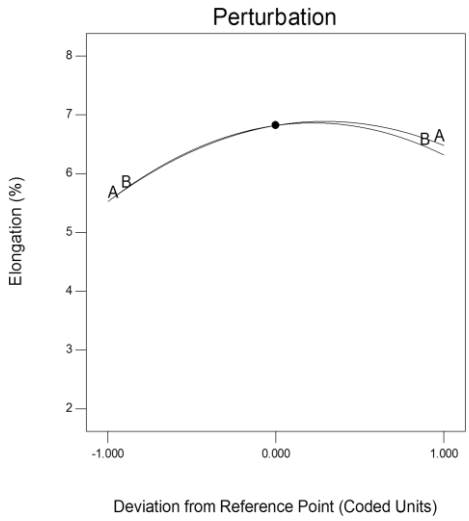

Figure 13: Perturbation of elongation showing the influence of each input factor over the selected level

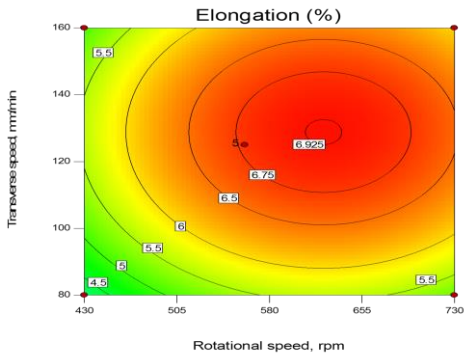

Figure 14: 2D plot depicting the effect of input factors on elongation

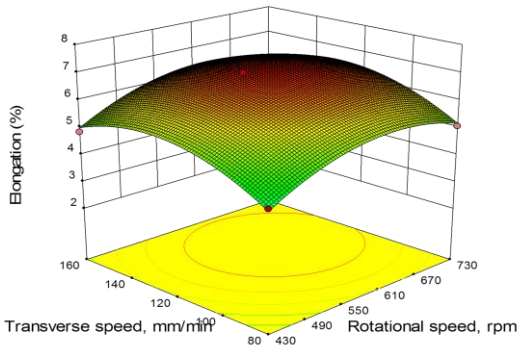

Figure 15: 3D plot revealing the influence of the input factors on elongation

Figure 16: a) Tunnel defect at lower rotational speed (V = 125 mm/min, Ω=340 rpm), b) Welding zone (V=125 mm/min, Ω=560 rpm), c) Void defect in the Welding zone (V=200 mm/min, Ω=560 rpm)

4.3 Modeling of the Ultimate Tensile Strength

Similarly, for the tensile strength, the (ANOVA) analysis for response surface quadratic model was completed to statistically analyze the outcomes, as listed in table (8). The model F-value of (309.75) in this table reveals that this model is significant. The experiment quadratic predicted model is given in terms of actual Factors as follows:

$$\text{Ultimate tensile strength} = -81.48221 + 0.48832 * A + 1.83173 * B - 3.59411E-004 * A^2 - 6.90682E-003 * B^2 \quad \ldots\ldots\ldots\ldots\ldots\ldots\ldots\ldots\ldots\ldots (2)$$

The diagnostic inspection of the model was performed by utilizing residual analysis. Similar to elongation model, the plot of normal probability for the tensile stress appeared that the residuals locate on a straight line revealing the normally distribution of the errors. Regarding the standardized residuals versus predicted data, these residuals did not depict any evident of unusual modality and they are distributed in both negative and positive sides. This reveals the accuracy of the model. Figure (17) manifests that the predicted data of tensile strength are near to the actual that were obtained from the trials, denoting a good harmony between the predicted and experimental outcomes. Concerning the individual influence of each input parameter deviated from the center point of the selected level, figure (18) indicates the perturbation of tensile strength in this model. Referring to influence of the interactions between the input process parameters, the result is also definite by the 2D contour plot and 3D surface graph depicted in Figures (19 and 20), in terms of welding and rotational speeds. Figure (19) provides the 2D contour plot of rotational and welding speeds and tensile strength as a response. At first, the increasing in the rotational speed leads to increase the tensile strength, then it decreased with the increasing the rotational speed. This behavior also applies to the welding speed. The explanation for this behavior is similar to that mention for the elongation. Figure (20) views the 3D plot of welding parameters influence on the tensile strength, and it can be observed that the rotational and welding speeds have a similar effect.

Table 7: ANOVA analysis for Response Surface Reduced Quadratic Model for Ultimate tensile stress

Source	Sum of Squares	Degrees of freedom	Mean Square	F Value	p-value Prob > F
Model	4419.16	4	1104.79	309.75	< 0.0001 significant
A-Rotational speed	1077.18	1	1077.18	302.01	< 0.0001
B-Welding speed	583.13	1	583.13	163.49	< 0.0001
A^2	1364.81	1	1364.81	382.65	< 0.0001
B^2	2784.09	1	2784.09	780.57	< 0.0001
Residual	28.53	8	3.57		
Lack of Fit	7.33	4	1.83	0.35	0.8358 not significant
Pure Error	21.20	4	5.30		
Cor Total	4447.69	12			
Std. Dev.	1.89		R-Squared		0.9936
Mean	183.65		Adj R-Squared		0.9904
C.V.	1.03		Pred R-Squared		0.9864
PRESS	60.52		Adeq Precision		50.228

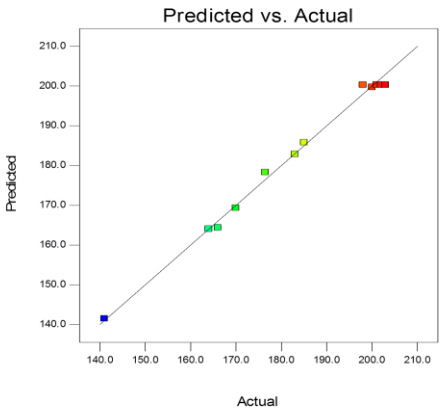

Figure 17: Predicted versus actual showing the ultimate tensile strength

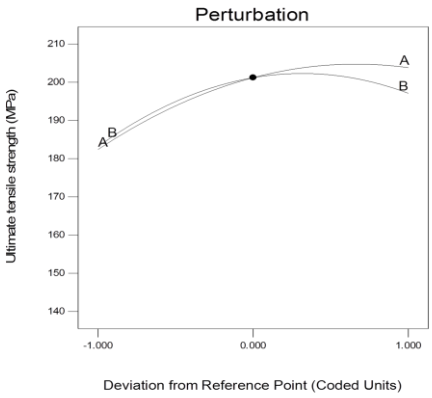

Figure 18: Perturbation of ultimate tensile strength showing the influence

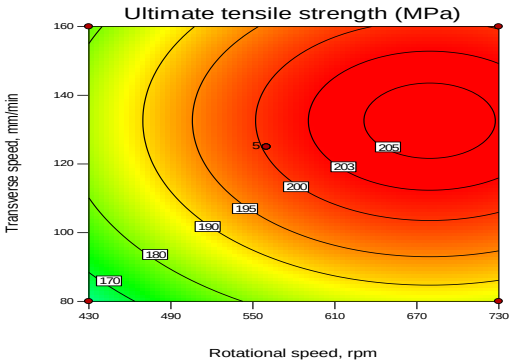

Figure 19: 2D plot depicting the influence of the input factors on ultimate tensile strength

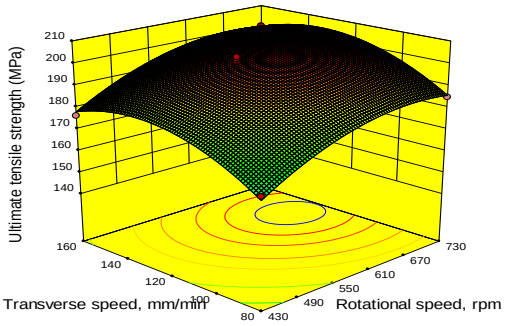

Figure 20: 3D plot revealing the influence of the input factors on ultimate tensile strength

4.4 Modeling of the Maximum Bending Force

Similarly, for the maximum bending force, the (ANOVA) analysis for response surface quadratic model was completed to statistically analyze the outcomes, as listed in table (9). The model F-value of (119.26) in this table reveals that this model is significant. The experimental quadratic predicted model is given in terms of actual Factors as follows:

$$\textbf{Maximum bending force} = -1.74148 + 0.014174 * \textbf{Rotational speed} + 0.046753 * \textbf{Welding speed} - 1.03913E-005 * \textbf{Rotational speed}^2 - 1.72555E-004 * \textbf{Welding speed}^2 \quad \text{(5.3)}$$

The diagnostic inspection of the model was performed by utilizing residual analysis. The plot of normal probability for the max. bending force showed that the residuals locate on a straight line revealing the normal distribution of the errors. Regarding the standardized residuals versus predicted data, these residuals did not exhibit any evidence of unusual modality and they are distributed in both negative and positive sides. This reveals the accuracy of the model, and there is no reason to think about any contravention of the assumption of independence or constant variance. Also, figure (21) manifests that predicted values of maximum bending force are close to actual that were obtained from the trials, denoting a good harmonization between the predicted and experimental outcomes. Concerning the individual influence of each input parameter deviated from the center point of the selected level, figure (22)

indicates the perturbation of max. bending force in this model. In connection with the influence of the interactions between the input process parameters, the consequence is depicted in figures (23 and 24), in terms of welding and rotational speeds. Figure (23) clarifies the 2D contour plot of rotational and welding speeds and max. bending force as a response, and indicates that the influence of welding parameters such as elongation and tensile strength models. Figure (24) illustrates the 3D plot of welding parameters influence on the max. bending force, it can be observed that the welding and rotational speeds have same effective.

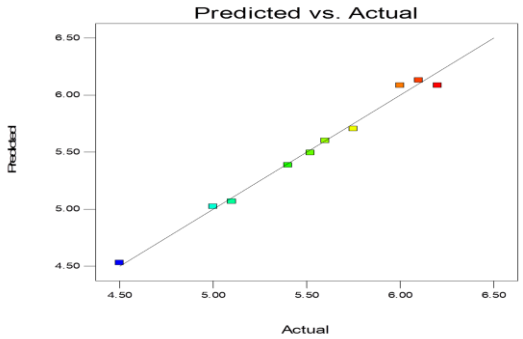

Figure 21: Predicted versus actual showing the maximum bending force data for comparison

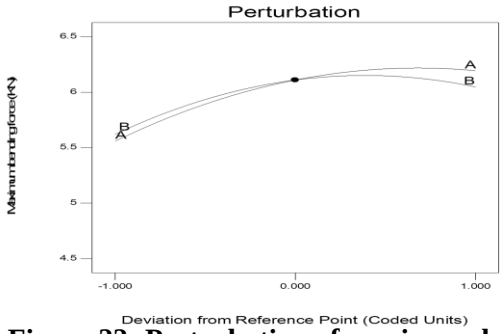

Figure 22: Perturbation of maximum bending force showing the influence of each input factor over the selected level

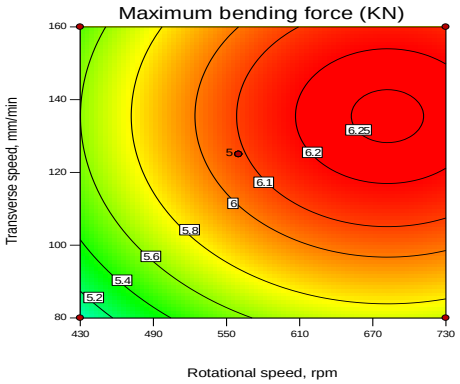

Figure 23: 2D plot depicting the effect of input factors on maximum bending force over the selected level

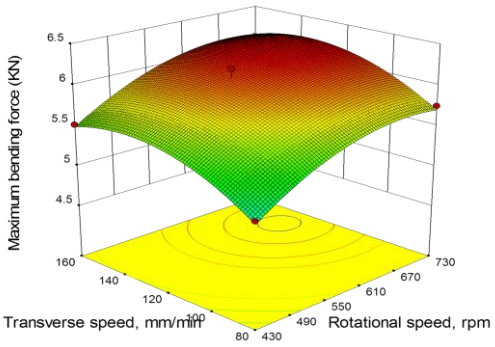

Figure 24: 3D plot revealing the effect of input factors on maximum bending force

Table 9: ANOVA analysis for Response Surface Reduced Quadratic Model for Maximum bending force

Source	Sum of Squares	DF	Mean Square	F Value	p-value Prob > F
Model	3.26	4	0.81	119.26	< 0.0001 significant
A-Rotational speed	0.95	1	0.95	139.04	< 0.0001
B-Transverse speed	0.55	1	0.55	80.30	< 0.0001
A^2	1.14	1	1.14	166.98	< 0.0001
B^2	1.74	1	1.74	254.33	< 0.0001
Residual	0.055	8	6.832E-003		
Lack of Fit	6.660E-003	4	1.665E-003	0.14	0.9591 not significant
Pure Error	0.048	4	0.012		
Cor Total	3.31	12			
Std. Dev.	0.083		R-Squared		0.9835
Mean	5.64		Adj R-Squared		0.9753
C.V.	1.46		Pred R-Squared		0.9673
PRESS	0.11		Adeq Precision		31.210

4.5 Numerical Optimization of Elongation, Tensile Strength and Maximum Bending Force

The numerical optimization is performed by the DOE program to detect the optimum sets of parameters for implementing the needs as wanted. Thus, this program is utilized for the optimization purpose, depending upon the data of predictive models for the outputs; elongation, tensile strength and maximum bending force as in terms of 2 input factors: rotational and welding speeds.

To build a new predicted model, a new objective function, called 'desirability' that permits the proper combination of all aims, was assessed. Desirability has to be maximized by a numerical optimization, and it takes a value from zero to one at the aim. The weight and importance of desirability are adjusted to change the features of the aim, and the optimization goal is to determine a proper combination of conditions that will satisfy all the aims. Normally, the weights are utilized to establish an assessment of the aim's 3D significance for maximizing the function of desirability; in the present research, weights are not varied, because the three outputs (elongation, tensile strength and maximum bending force) possess the main significance and are not in clash with each other.

The maximum aim of optimization was to find the peak output that met all the variable properties at the same time. Constrains of each parameter for numerical optimization of the elongation, tensile strength and maximum bending force are given in Table (10), showing one likely run satisfied these stated constrains to determine the optimum values of elongation, tensile strength and max. bending force, which are listed in Table (11). For this run, it is observed that the maximum selected desirability is (0.995). Figure (25.a) depicts the optimum value of the elongation in 3D surface plot (6.933%), while figure (25.b) illustrates the optimum value of the tensile strength (204.629 MPa), and figure (25.c) displays the optimum value of maximum bending force (6.216 KN).

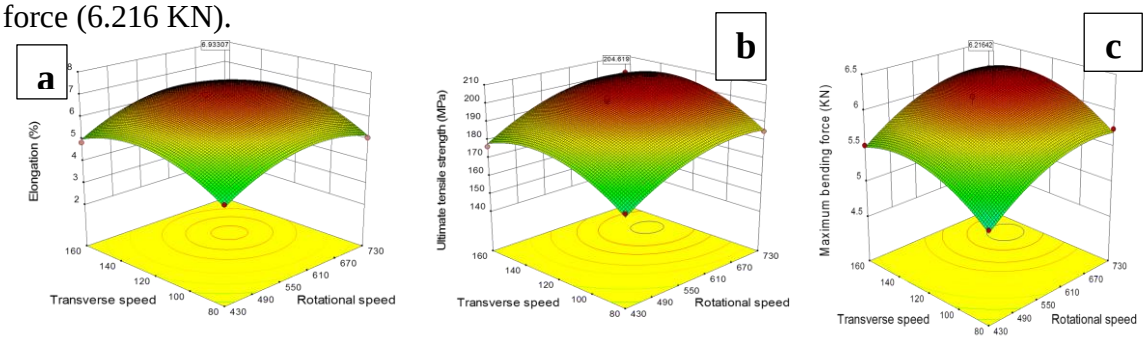

Figure 25: a) 3D plot depicting the max. elongation at the optimum conditions, b) 3D plot revealing the max. ultimate tensile strength at the optimum conditions, c) 3D plot manifesting the max. bending force at the optimum conditions

4.6 Confirmation Test

A confirmation test was performed so as to check the validity of the optimum solution experimentally. This test was carried out at the obtained input parameters (630 rpm rotational speed and 125 mm/min welding speed) according to the available speeds in the used milling machine to obtain the elongation, tensile strength and maximum bending force. The experimental values of these measurements are listed together with the predicted values in table (12) for comparison purposes. This table points out that there is a good agreement between the predicted and experimental results with a maximum error of 1.54 % for elongation, 2.26 % for ultimate tensile strength and 0.55% for maximum bending force. The curves of bending and tensile tests of the samples of the confirmation trial joint are shown in figures (15) and (16).

Table 9: Constraints of the optimization of elongation, ultimate tensile stress and maximum bending force

Name	Goal	Lower Limit	Upper Limit	Lower Weight	UpperWeight	Importance
A:Rotational speed	is in range	430	730	1	1	1
B:Transverse speed	is in range	80	160	1	1	1
Elongation	maximize	2.34	7	1	1	1
Ultimate tensile strength	maximize	141	203	1	1	1
Maximum bending force	maximize	4.5	6.2	1	1	1

Table 10: Optimum solution for maximum elongation, ultimate tensile stress and maximum bending force

Rotational speed(rpm)	Transverse speed (mm/min)	Elongation (%)	Ultimate tensile stress (MPa)	Maximum bending force (KN)	Desirability
623.949	128.795	6.933	204.629	6.216	0.995 selected

Table 11: Comparison between the experimental and predicted results

	Rotational speed (rpm)	Welding speed (mm/min)	Elongation (%)	Ultimate tensile stress (MPa)	Maximum bending force (KN)
Experimental	630	125	7.1	201	6.25
Predicted	623.949	128.795	6.933	204.629	6.216
% Error	------	------	1.54	2.26	0.55

Figure 26: Load-Deformation Diagram (bending force)

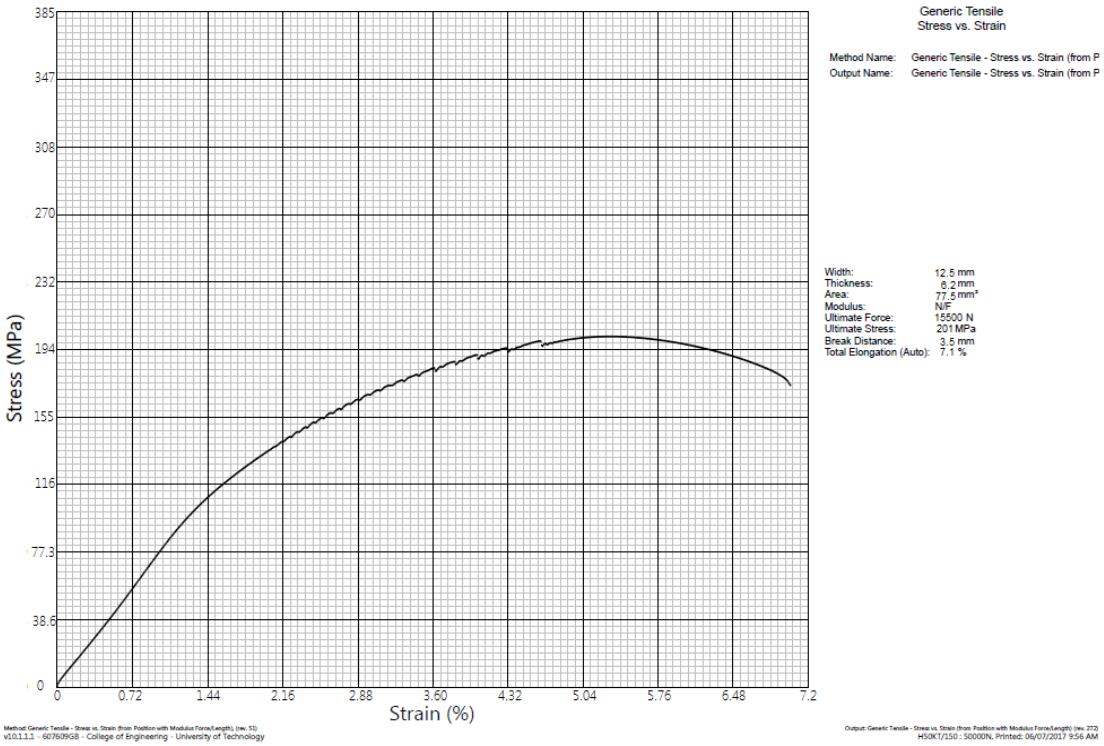

Figure 27: Tensile Stress-Strain Curve

5. Conclusions

The following conclusions have been based on the results of this work:

1- The outcomes of ANOVA appear that the models (mathematical relationships) can effectively presage the elongation, ultimate tensile strength and maximum bending force of the BFS welded joints with 95 % level of confidence.

2- For elongation, ultimate tensile strength and maximum bending force of welded joints, the effects of welding and rotational speeds are most significant.

3- Increasing of the welding speed to (125 mm/min) first leads to raise the mechanical properties of welded joints to maximum values and then drops them because of the void formation.

4- As the rotational speed rises, the mechanical properties of welded joint first increases and then decreases.

5- From numerical optimization, the optimum results of elongation, ultimate tensile strength, and maximum bending force are found to be (6.933%), (204.629 MPa) and (6.216 KN), respectively, with a desirability 0.995 at (128.795 mm/min) welding speed and (623.949 rpm) rotational speed.

6- The confirmation test at a rotational speed of (630 rpm) and a welding speed (125 mm/min) gave better elongation (7.1), ultimate tensile strength (200 MPa) and maximum bending force (6.25 KN) with a maximum error of 2.26%.

References

ASTM, 1991,"Heat treatment of Tool steels, Heat Treating", ASM, Vol. 4.

ASTM A681-94, 2004, "Standard Specification for Tool Steel Alloy", ASTM A681-94

ASTM B209, 2004, "Standard Specification for Aluminum and Aluminum Alloy ASTM Sheet and Plate".

ASTM E190M, 2004, "Standard Method for Guided Bend Test for Ductility of Welds".

ASTM E8M, 2004, "Standard Test Method for Tension Testing of Metallic Materials", ASTM E8M.

Cevik B., Y. Ozcatalbas and B. Gulence, 2016, "Effect of welding speed on the mechanical properties and weld defects of 7075 Al alloy joined by FSW", Kovove Mater., Vol. 54, pp. 241-247.

Fonda R.W. and Bingert J. F. , 2004, Microstructural evolution in the heat-affected zone of a friction stir weld. Metal Mater Trans.,Vol. 35, pp. 1487–99.

Ghetiya N. D. and Patel K. M. , 2014, "Prediction of Tensile Strength in Friction Stir Welded Aluminum Alloy Using Artificial Neural Network," Procedia Technol., Vol. 14, pp. 274–281.

Jayaraman M., R. Sivasubramanian, V. Balasubramanian, and A. K. Lakshminarayanan, 2009, "Optimization of process parameters for friction stir welding of cast aluminum alloy A319 by Taguchi method," J. Sci. Ind. Res. (India)., Vol. 68, No. 1, pp. 36–43.

Kumbhar N. T., and Bhanumurthy K. , 2008, "Friction stir welding of Al 6061 alloy", Asian J. Exp. Sci., Vol. 22, pp. 63-74.

Li W.Y., T. Fua, L. Hütsch, J. Hilgert, F.F. Wang, J.F. dos Santos and N. Huber, 2014, "Effects of tool rotational and welding speed on microstructure and mechanical properties of bobbin-tool friction-stir welded Mg AZ31," Mater., Vol. 64, pp. 714–720.

Liu H. J., J. C. Hou and H. Guo, 2013, "Effect of welding speed on microstructure and mechanical properties of self-reacting friction stir welded 6061-T6 aluminum alloy", Materials and Design, Vol. 50, pp. 872–878.

Mishra R. S. and Ma Z. Y. , 2005, "Friction stir welding and processing", Materials Science and Engineering, R 50, pp. 1–78.

Mishra R. S., P. S. De and N. Kumar, 2014, "Friction Stir Welding and Processing Science and Engineering", Springer.

Montgomery, D. C. , 2000, "Design and Analysis of Experiments", 5th Edition, John Wiley & Sons Inc..

Samir A. Al-rubaie, Q. A. Atiah and Z. Altaher, 2015, "Determination of Optimum Welding Parameters for FSW AA2024-T351," Al-Khwarizmi Eng. J., Vol. 11, No. 1, pp. 51–64.

Sato Y. and Kokawa H. , 2001, "Distribution of tensile property and microstructure in friction stir weld of 6063 aluminum", Metall. Trans, . A 32, pp. 3023–3031.

Sued M. K. and Pons Dirk J. , 2016, "Dynamic Interaction between Machine, Tool, and Substrate in Bobbin Friction Stir Welding", International Journal of Manufacturing Engineering, Article ID 8697453, 14 pages.

Sued M. K., D. Pons, J. Lavroff, and E. H. Wong, 2014, "Design features for bobbin friction stir welding tools: Development of a conceptual model linking the underlying physics to the production process", Materials and Design, Vol. 54, pp. 632–643.

Threadgill P. L., M. M. Z Ahmed, J. P. Martin, J. G. Perrett and B. P. Wynne, 2010, "The use of bobbin tools for friction stir welding of aluminum alloys", Materials Science Forum, Vol. 638-642, pp. 1179-1184.

Trueba L., M. A. Torres, L. B. Johannes, and D. Rybicki, 2017, "Process optimization in the self-reacting friction stir welding of aluminum 6061-T6," Int. J. Mater. Form., Vol. 9, pp. 1-12.

Wang F. F., W. Y. Li, J. Shen, S. Y. Hu, and J. F. dos Santos, 2015, "Effect of tool rotational speed on the microstructure and mechanical properties of bobbin tool friction stir welding of Al-Li alloy," Mater., Vol. 86, pp. 933–940.

Zhang H., M. Wang, X. Zhang, and G. Yang, 2015, "Microstructural characteristics and mechanical properties of bobbin tool friction stir welded 2A14-T6 aluminum alloy," Mater. Des., Vol. 65, pp. 559–566.

Zhou L., G. H. Li, C. L. Liu, J. Wang, Y. X. Huang, J. C. Feng and F. X. Meng, 2017, "Effect of rotation speed on microstructure and mechanical properties of self-reacting friction stir welded Al-Mg-Si alloy," Int. J Adv. Manuf. Technol., Vol. 89, pp. 3509-3516 .